Identification of structures capable of hosting the M_L 5.5 Orkney South Africa earthquake and factors controlling the physics and mechanics of dynamic rupture

by S.B. Mngadi[1,4], M.S.D. Manzi[1,4], N.Z. Nkosi[1,4], R.J. Durrheim[1,4], Jr.H. Ogasawara[2,4], Y. Yabe[3,4], DSeis team[4]

Affiliation:
[1]School of Geosciences, University of the Witwatersrand, South Africa
[2]College of Science and Engineering, Ritsumeikan University, Japan
[3]Graduate School of Engineering, Tohoku University, Japan
[4]The International Continental Scientific Drilling Program (ICDP) Dseis team

Correspondence to:
S.B. Mngadi

Email:
siyanda.b.m@gmail.com

Dates:
Received: 5 Jun. 2024
Revised: 22 Dec. 2024
Accepted: 21 Jan. 2024
Published: January 2025

How to cite:
Mngadi, S.B., Manzi, M.S.D., Nkosi, N.Z., Durrheim, R.J., Ogasawara, Jr.H., Yabe, Y., DSeis team. 2025. Identification of structures capable of hosting the M_L 5.5 Orkney South Africa earthquake and factors controlling the physics and mechanics of dynamic rupture. *Journal of the Southern African Institute of Mining and Metallurgy*, vol. 125, no. 1, pp. 33–42

DOI ID:
http://dx.doi.org/10.17159/2411-9717/3445/2025

ORCiD:
S.B. Mngadi
http://orcid.org/0000-0001-6611-4690
M.S.D. Manzi
http://orcid.org/0000-0002-1654-5211
M.S.D. Nkosi
http://orcid.org/0009-0007-0285-8480
R.J. Durrheim
http://orcid.org/0000-0003-3832-0600
Y. Yabe
http://orcid.org/0000-0003-0256-1904

Abstract

On 5 August 2014, the Orkney M5.5 earthquake, the largest in South African gold mining districts, occurred with an unusual strike-slip mechanism at great depth of 4.78 km below the surface. In a rare case, the M_L 5.5 earthquake occurred within the area covered by the legacy 2D and 3D reflection seismic data acquired in the 1990s and 2000s for gold exploration and mine development. In addition, the earthquake M_L 5.5 rupture plane was recorded and accurately delineated by the underground in-mine seismic network near the source region. The integration of the legacy 2D reflection seismic data and mine seismicity data allowed us to identify a near-vertical structure, striking northnorthwest-south southeast (NNW-SSE). The ICDP-DSeis team drilled three holes (Hole A, Hole B, and Hole C), and two holes (Hole B and Hole C), intersected the upper edges of the M_L 5.5 rupture. These holes recovered metasediments, metabasalts, intrusive rocks including dolerite sills and lamprophyre dykes adjacent to the fault zone, and the fault gouge. Late Prof. Tullis Onstott and geomicrobiologists installed a packer in Hole A and successfully recovered saline water and detected gas (~10 MPa). Slip weakening and rupture propagation are significantly influenced by the existence of fault gouges and the production of wear material between two sliding rock surfaces. Using the fault gouge material recovered from Hole C, we conducted friction experiments under dry and room temperature conditions at high slip velocity of ~100 mm/s and normal stress of 2 MPa. The resulting steady-state frictional strength was ~0.66 over a slip weakening distance of ~9.1 m. The steady-state frictional strength was high, which may be caused by large gouge thickness, and the rate of wear generation. As a result, it is proposed that the Moab Khotsong M_L 5.5 seismogenic zone is complex and could be controlled by three main processes: a) the complex structural architecture of the seismogenic zone (e.g., intersection of fault, lamprophyre dykes, and dolerite sills); b) the mechanical process induced by tectonic and/or mining related stresses; and c) the mechanical and chemical processes caused by the water and rock interaction.

Keywords

seismicity, seismics, mining, friction experiments, fault gouge, structures

Introduction

Mining at deep levels in highly stressed rock mass may induce earthquakes and pose risk to the life of workers, mine infrastructure, and the public. The study area is located under the Moab Khotsong mine at a depth of 4.78 km below surface (Figure 1), where the largest earthquake recorded in the Witwatersrand Basin, South Africa, occurred in 2014 with a local magnitude of M_L 5.5. The vibrations caused by this seismic event were 'felt' across South Africa and some neighbouring countries, e.g., Mozambique, with one recorded death (Midzi et al., 2015). The assessed damage was valued at ~R130 million (USD 8.6 million) (Midzi et al., 2015). Though these large seismic events may result in damage and loss of life, they also provide a rare opportunity to study the physics and mechanisms of earthquakes near source regions, which may enhance our understanding of seismic hazard and mitigation strategies (Durrheim, 2012).

This M_L 5.5 earthquake prompted seismologists, in particular the ICDP - DSeis team of the International Continental Scientific Drilling Programme, who are drilling into seismogenic zones of M_L 2.0 – 5.5 earthquakes in deep South African gold mines, to pose a few fundamental research questions relevant to this study: (1) what is the nature of fault rock that hosted the M_L 5.5 earthquake? (2) what is the role of geology? and (3) what is the geological structure (fault, dyke, or sill) related to this earthquake? (Ogasawara et al., 2019). The ICDP - DSeis team drilled into a number of active faults. These seismogenic

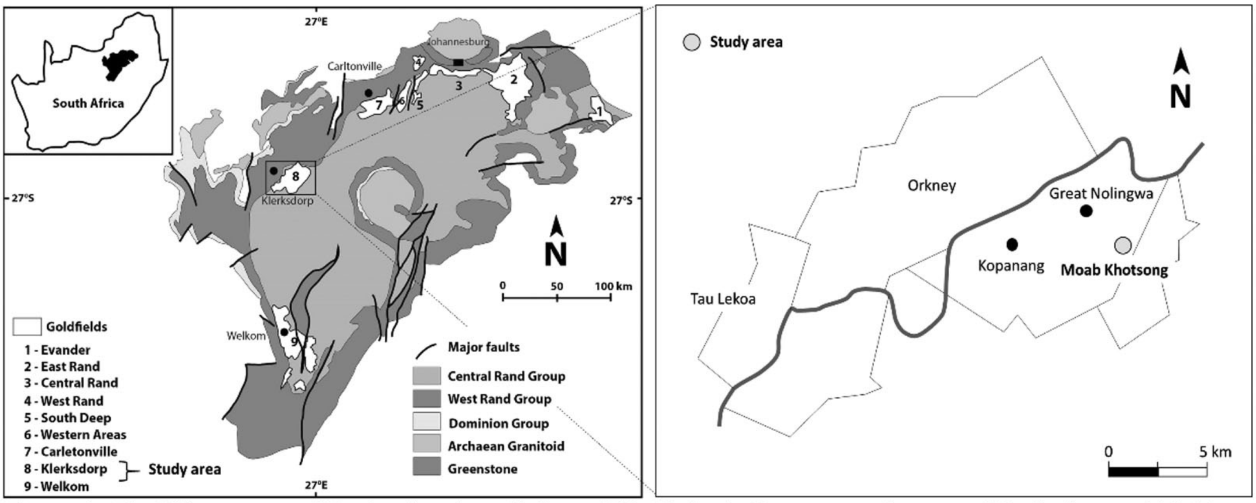

Figure 1—The Witwatersrand Basin showing all the goldfields including our study area – Klerksdorp goldfields, Moab Khotsong mine (modified from Dankert and Hein, 2010)

zones are situated at deep level and highly stressed rock mass in South African gold mines, including the Moab Khotsong M_L 5.5 earthquake rupture. The Moab Khotsong M_L 5.5 seismic event occurred at 4.78 km, which is 1.78 to 2.78 km below the mining levels situated between 2.0 and 3.0 km depth. The faulting mechanism was characterised as strike-slip (Ogasawara et al., 2017). This was distinct from the common 'normal faulting' mechanism associated with mining-induced activities in this region. This study forms a portion of a greater ICDP-DSeis project. The broader aims of the ICDP-DSeis project include the investigation of the extent of damage, the stress state around the fringes of the earthquake, and the potential existence of living organisms associated with deep-level earthquakes. The ICDP-DSeis team comprises international researchers from South Africa, Japan, Germany, Switzerland, the USA, Israel, and India. The DSeis team completed drilling at Moab Khotsong to intersect the M_L 5.5 rupture and recovered fragile fault rocks (Ogasawara et al., 2017). In this study, we focus on the identification of structures capable of hosting the M_L 5.5 Orkney, South Africa, earthquake, and investigating the fault rock composition, frictional properties, and the architecture of the 'unusual' strike-slip fault in deep mines.

Mine seismicity

Unique to this study, is that the M_L 5.5 earthquake was recorded with a dense and high resolution in-mine seismic network. The in-mine seismic network consisted of 46 triaxial geophones with a frequency of 4.5 Hz and a sampling rate of 6 kHz. The geophones were located near the M_L 5.5 earthquake at mining levels between depths of 2.0 km and 3.5 km (Imanishi et al., 2017). Using this dense in-mine seismic network, which is located near the source region, more than 2000 foreshocks and aftershocks were recorded from 4 August 2014 to 31 October 2014, which included the mainshock (M_L 5.5 earthquake) (Figure 2). The velocity field used to process and locate these seismic events, also routinely used at Moab Khotsong mine, is the P-wave velocity of ~5960 m/s and the S-wave velocity of ~3610 m/s. The depth of the mainshock was located at ~ 4.78 km below surface. The delineated aftershock distribution spanned ~ 8 km in strike length and ~3 km in dip length. The distribution of these aftershocks revealed that the M_L 5.5 rupture plane dips near vertical and strike in a northnorthwest-southsoutheast (NNW-SSE) direction, with strike-slip fault mechanism (Imanishi et al., 2017; Ogasawara et al., 2018).

Imanishi et al. (2017) reported that the M_L 5.5 earthquake triggered seismicity at the mining levels. However, to the authors' knowledge, no seismic rupture was observed or mapped in the mining levels. This could mean that the main rupture did not propagate to the mining levels. Therefore, the geological structure responsible for M_L 5.5 earthquake remains elusive and not clearly understood. In addition, the aftershock plane, when projected to the mining levels, did not match any known fault or geological structures that could have hosted the M_L 5.5 earthquake (Ogasawara et al., 2018).

Legacy reflection seismic data

Coincidentally, the M_L 5.5 seismic event occurred in the mining region that is well covered by the several 3D and 2D seismic reflection data originally acquired for mineral exploration (Figure 2a and Figure 3). The shot gathers of legacy 2D reflection seismic profiles were analysed, and only profile AV01 was selected for reprocessing and interpretation due to its ideal perpendicular position to aftershocks (Figure 3). This profile (AV01) was acquired by Anglo Gold Ashanti in 1992, using the vibroseis trucks as energy sources at linear sweep frequency of 10 Hz – 90 Hz with sweep length of 16 s, sampling rate of 2 ms, and recording length of 6 s. The source and receiver (10 Hz) intervals were 50 m and 25 m, respectively. These 2D seismic reflection data were reprocessed using a post-stack migration standard workflow (Manzi et al., 2012a), mainly focusing on improving the velocity analysis guided by the laboratory ultrasonic measurements. Nkosi et al. (2022) conducted physical property measurements of cylindrical core specimens that were retrieved from the ICDP-DSeis project (Hole A, Hole B, and Hole C). The results were compared with downhole physical property data (e.g., sonic and density). The measured rock specimens included intrusives, metasediments, and metabasalts. Subsequently, the data were interpreted to examine and characterise the geological structure that hosted the Orkney earthquake M_L 5.5.

Geology of Moab Khotsong mine

Witwatersrand Supergroup

The geology of the Archaean Witwatersrand Basin has been described in detail by several researchers since the gold rush in 1886 (Robb and Meyer, 1995; McCarthy and Rubidge, 2005; Dankert and Hein, 2010). The Witwatersrand Supergroup comprises two groups,

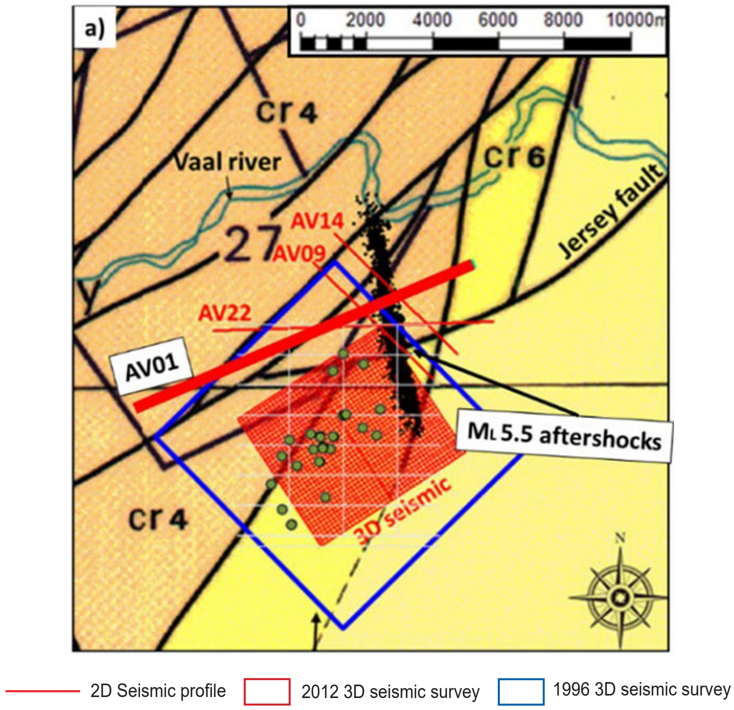

Figure 2—Shows legacy reflection seismic surveys including 1996 3-D survey (blue), 2012 3-D survey (red), and selected 2-D seismic reflection profile (AV01) in relation to aftershocks (black), structures (black) (Modified from Ogasawara Jr. et al., 2018)

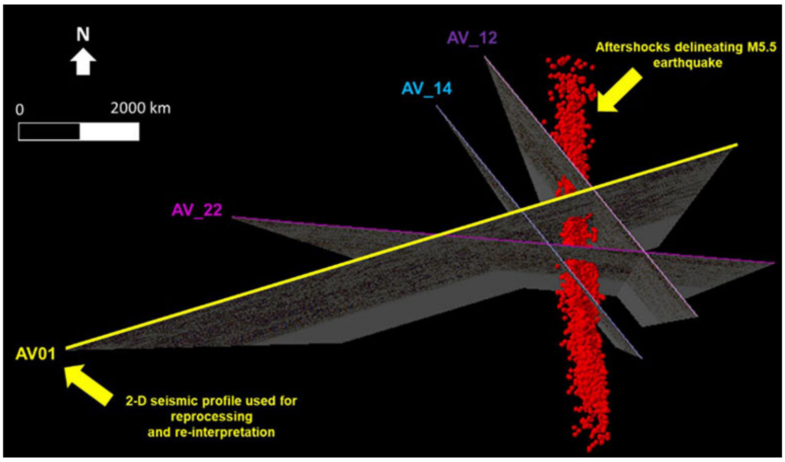

Figure 3—Several 2D legacy seismic profiles are shown (AV01, AV_12, AV_14 and AV_22). After short gather analysis, only seismic profile AV01 was reprocessed and reinterpreted. This reflection seismic profile is almost perpendicular to the aftershock plane

namely the West Rand Group and the Central Rand Group (Myers et al., 1989; Robb and Meyer, 1995; Dankert and Hein, 2010). The West Rand and Central Rand groups tend to decrease in thickness towards the south-eastern edges of the basin. The average thickness of the basin is ~ 4.6 km. The West Rand Group is dominated by clastic sedimentary rocks, such as quartzites and shales with a ratio of about 1:1, and conglomerate 'primarily mined for gold'. The Central Rand Group hosts more than 70% of the gold-bearing conglomerate horizons and lies on top of the West Rand Group. The Central Rand Group also consists of quartzite and conglomerate packages, and minor bands of shale and lavas (SACS, 1990). The Vaal Reef is the major gold-bearing conglomerate exploited at Moab Khotsong mine and neighbouring mines, such as Kopanong and Great Nolingwa.

Faults, dykes, and sills

The Witwatersrand Basin is structurally complex and has undergone several episodes of deformations. The basin generally exhibits major listric normal faults and their related drag folds that are ascribed to the extensional tectonic regime during the deposition of the Ventersdorp Supergroup (Vermaakt and Chunnet, 1994; Coward et al., 1995). Watts (2005) conducted a detailed mapping of faults with vertical displacements in excess of 10 m at the neighbouring Kopanong mine. They can be grouped into two main categories (1) Zuiping-type faults, and (2) Jersey-type faults. Watts (2005) concluded that most of these faults are Platberg age. The Platberg volcanism occurred at 2754-2709 Ma (Gumsley et al., 2020).
Our study area is characterised by numerous sills and dykes that intruded at different geological ages and have been subjected to

several damaging brittle seismic events (Yabe et al., 2019). The sills and dykes are of different ages, such as known post-Karoo dykes of pre-Cretaceous and Cretaceous age (145 - 66 Ma), Karoo dykes (150 Ma), Pilanesberg (1.30 Ga), Transvaal (2.20 Ga), and Ventersdorp (2.60 Ga). These intrusive rocks often host large damaging seismic events (M3.0-3.9) (Van der Heever, 1982) and therefore, are important to understand for mine design and during mining operations (Ogasawara et al., 2019; Yabe et al., 2019).

Moab Khotsong mine drilling: Hole A, B, and branch Hole C

The ICDP-DSeis team drilled three holes, labelled as Hole A, Hole B and Hole C, into the M_L 5.5 earthquake rupture delineated by the aftershocks recorded by the in-mine seismic network (Figure 4a). The drilling was, in part, conducted to recover fault rocks and gouge material. Before drilling could take place, the ICDP-DSeis team excavated the chamber by enlarging a portion of a tunnel located at a depth of 2.9km. The dimensions of the drilling chamber are 6m x 6m x 6m. The mine safety regulations did not allow for larger excavation dimensions. The ICDP-DSeis team successfully drilled and recovered fragile ruptured core and fault gouge material. The drilling plunged at 35°–45° downward from the excavated drilling site.

Hole A deflected too much, hence, it could not intersect the M_L 5.5 rupture plane, and it was terminated at 817 m. However, Hole A provided a stable hole with good core recovery, allowing the ICDP-DSeis team to measure rock physical properties, conduct borehole geophysical logging, and measure stress variations near the aftershock region. Additionally, Onstott and other geomicrobiologists investigated gas, water, and biomass by installing the automated system for sampling water and gas. The group successfully collected saline water by installing a packer (~10 MPa at the packer) in Hole A at a depth near 420 m, and detected gas (Ogasawara et al., 2020).

The deflection of Hole A led to the drilling of Hole B with a modified by 15° angle (Figure 4b) (Ogasawara et al., 2020). Hole B intersected the uppermost part of the M_L 5.5 rupture zone, experiencing a 3 m core-loss zone using a 'double tube' core barrel. The drilling was terminated at 700 m from the collar after intersecting the rupture zone, encountering core-loss and instability. Because the important part of the core was lost, i.e., fault gouge material and core samples, the team drilled a branch hole (Hole C) using a 1.5 m 'triple tube' core barrel. Hole C started at 544 m of Hole B and completed at 640 m. The 1.5 m triple tube core barrel drilling technique successfully recovered core samples and fragile fault gouge material.

Hole B and Hole C intersected an altered lamprophyre dyke and the subsequent core-loss zone (Figure 5). The location of the dyke and core-loss zone in the drill core corresponds to the location of the aftershock plane, which was delineated from M_L 5.5 earthquake. This suggests that the dyke might be the geological structure that hosted the M_L 5.5 rupture. The drilling programme was immediately followed by detailed core logging and downhole geophysical borehole logging of Hole A. The geophysical borehole logging included density and seismic velocity measurements, which showed high seismic velocities coinciding with intrusive rocks compared to other rocks (Figure 6). This suggests that intrusive rocks should have higher acoustic impendence contrast relative to the country rocks (Nkosi et al., 2022). For recovered core from Hole A, Yabe et al. (2019) performed non-destructive stress measurements and an analysis on the core and revealed that stress concentration coincided with the intrusive rock at ~440 m from the borehole collar (Figure 6). A different zone of stress concentration was observed at the depth or location of the upper part of the aftershock plane. The core was sampled at selected lithological units for X-ray diffraction (XRD) analysis.

Minerals and friction experiments

The mineral composition of the fragile core material recovered from Hole B and Hole C was examined. This is because the mineralogy of the fault material has an impact on the mechanical behaviour, the frictional strength, and dynamic rupture propagation. An XRD analysis was conducted on the lamprophyre dykes and fault gouge material, and the results are presented in the following.

XRD analysis

Lamprophyre dykes

The dominant minerals found in the intrusive rock (lamprophyre dykes), which is thought to host the M_L 5.5 earthquake, are biotite (25.06–29.62 wt%), talc (22.60–37.05 wt%), actinolite (16.79–23.11wt%), diopside (4.04–14.43 wt%), chlorite (5.00–7.46 wt%), kaolinite (3.40–4.77 wt%), calcite (1.02–4.30 wt%), and quartz (0.37–0.83 wt%).

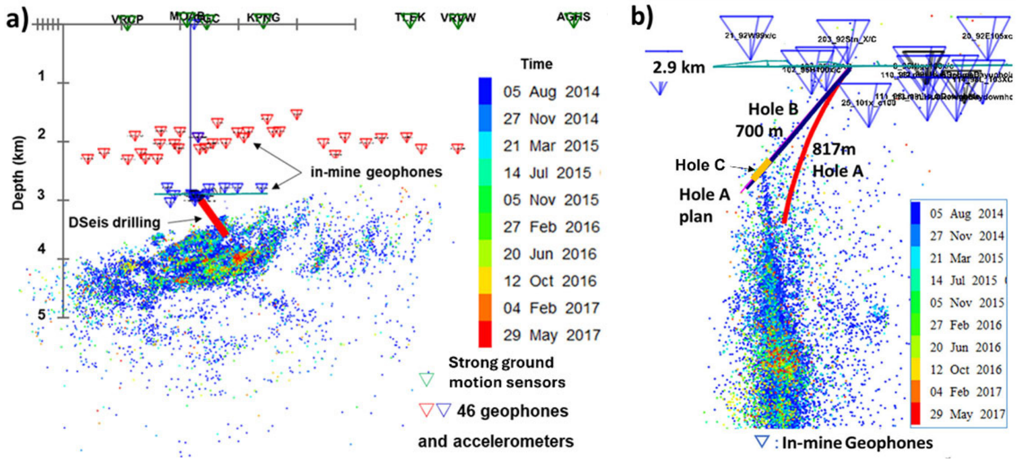

Figure 4—(a) Location of aftershocks generated by M_L 5.5 earthquake delineating the rupture plane. (b) Location of Hole A, Hole B and Hole C, where Hole B and Hole C intersected the rupture and intrusive rock potentially responsible for the M_L 5.5 event (Ogasawara et al., 2019)

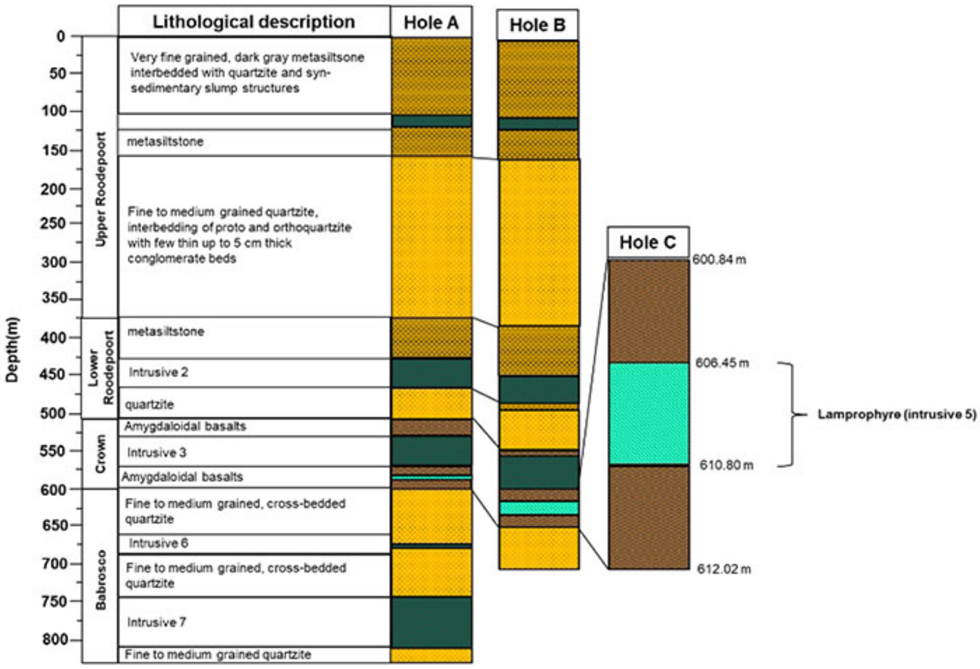

Figure 5—The core logging descriptions of Hole A and B were first conducted by Rickenbacher (2018). In this study we largely focused on the branch Hole C (not illustrateded to scale)

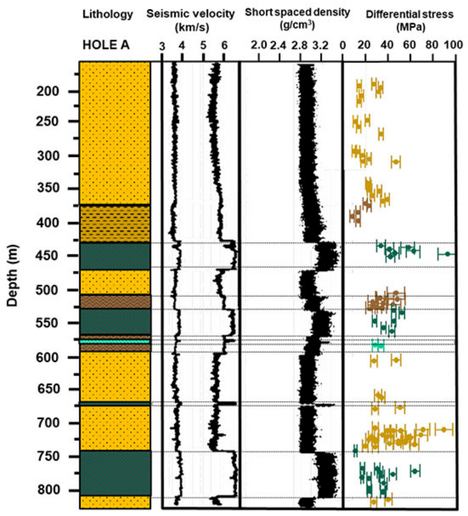

Figure 6—The lithological units described from core logging and geophysical borehole logging (Rickenbacher, 2018). Yabe et al. (2019) used diametrical core deformation analysis (DCDA) to measure insitu rock differential stress. The description of the lithology is provided in Figure 5 (Ishida et al., 2018)

Fault gouge

The gouge material was sampled at 63 m (branch Hole C), i.e., equivalent to 608 m distance from the borehole collar of Hole B (see Figure 5), around the core loss zone. Approximately, 3 – 4 g of the gouge material was sampled for XRD analysis. The XRD results of the gouge material are shown in Table 1.

Friction experiments

In earthquake physics, friction is crucial because it affects the propagation of ruptures and the weakening of faults. Frictional resistance weakens exponentially with increasing slip displacement during rupture propagation, namely slip weakening behaviour. The slip weakening behaviour is described by the exponential decay equation (Mizoguchi et al., 2007):

$$\mu = \mu_r + (\mu_i - \mu_r)\, e^{\left(\frac{\ln(0.05)*d}{d_c}\right)} \qquad [1]$$

where, μ is the frictional coefficient, μ_i is the peak friction coefficient (frictional resistance), μ_r is the steady-state friction coefficient, and d is displacement. The exponential decay equation decreases friction to a constant value, as displacement approaches infinity, thus, one defines d_c as a displacement, where (μ_i-μ_r) decreases to ~5% of (μ_i-μ_r), and lets d_c represent D_c. This means d_c represents a critical slip displacement (D_c), which is defined as the weakening of the frictional resistance over slip weakening displacement during rupture propagation (Mizoguchi et al., 2007).

The fault gouge material was collected from the M_L 5.5 rupture at Moab Khotsong mine and used to perform high slip velocity (100 mm/s) friction experiments. The fault gouge material was sheared at an applied normal stress of ~2 MPa. The fault gouge

Table 1

XRD analysis of recovered Moab fault gouge from the Orkney M5.5 event (Hole C at depth of ~608 m)

Sample no.	Calcite (wt%)	Quartz (wt%)	Biotite (wt%)	Actinolite (wt%)	Chlorite (wt%)	Talc (wt%)	Sepiolite (wt%)	Total (wt%)
Moab fault (1)	13.31	1.76	20.06	33.97	9.77	20.86	0.27	100
Moab fault (2)	11.98	1.56	20.09	32.57	11.33	22.03	0.44	100

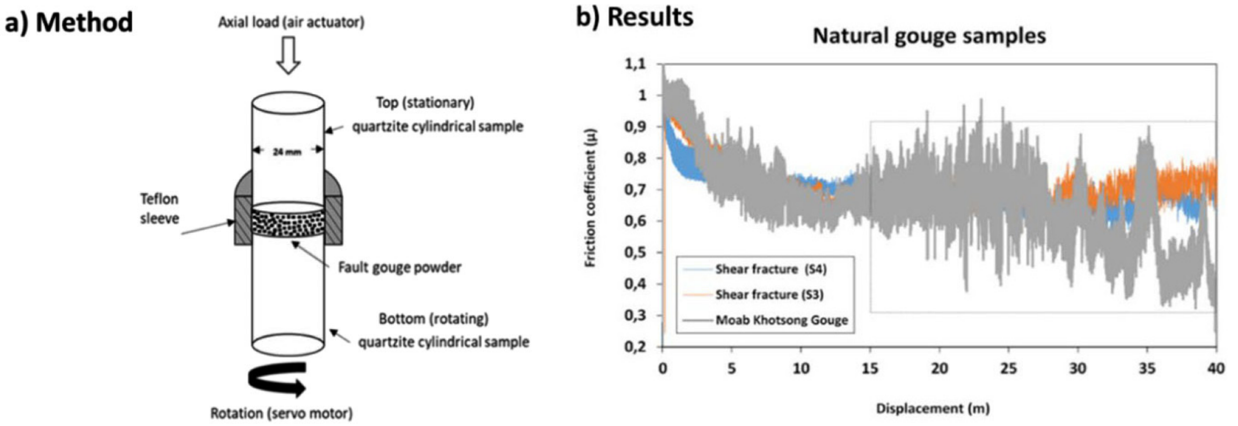

Figure 7—(a) A graphic illustration of the sample assembly for high-velocity friction experiments conducted with an intervening gouge material recovered from the M_L 5.5 earthquake (modified from Mngadi et al., 2021). (b) The friction weakening behaviour of the Moab Khotsong mine strike slip fault gouge (grey), in comparison with the fault gouge samples recovered from the normal faults (M1-4) occurring ahead of the stope at Cooke 4 mine

Table 2

The peak (μ_p) and steady (μ_s) state friction coefficient of the Orkney M5.5 earthquake compared to Ortlepp shear fractures at 100 mm/s slip velocities (V_{eq}) and 2 MPa normal stress over defined slip weakening distance D_c

	V_{eq} (mm/s)	Normal stress (MPa)	μ_p	μ_s	D_c (m)
Moab Gouge	100	2	1.0	0.66	9.15
Shear fracture S(3)	100	2	0.92	0.71	6.1
Shear fracture S(4)	100	2	0.98	0.67	12.8
Artificial Gouge	100	2	0.97	0.69	9.6

sample (weight of ~1 g, equivalent to ~1 mm gouge thickness) was used as an intervening layer between two sliding rock surfaces (Figure 7a). The sliding rock quartzite cylinders and a Teflon sleeve were used to prevent the fault gouge from leaking during shearing. The friction experiments were conducted under room-dry conditions. The fault gouge reached a peak friction coefficient of ~1.0 that decreased to steady-state friction of ~0.66 at ~ 100 mm/s slip velocities. This weakening occurred over a slip weakening distance of ~9.1 m.

Furthermore, Mngadi et al. (2021) used gouge material (S(3) and S(4)) recovered from Cooke 4 mine brittle shear fractures (also known as Ortlepp shear) occurring at the mining levels (M1-4) to make a comparison between these results and similar work on friction experiments in South African deep mines. These shear fractures have normal faults mechanism. The experiments were conducted under similar conditions at slip velocity of 100 mm/s and normal stress of 2 MPa, but different gouge material thicknesses of ~0.5 mm. Sample S(3) revealed peak friction of ~0.98, which weakened to steady-state friction of ~0.67 over a slip weakening displacement of ~12.8 m (Mngadi et al., 2021). Sample S(4) revealed peak friction of 0.92, which weakened to steady-state friction of 0.71, over a slip weakening displacement of ~6.1 m (Mngadi et al., 2021) (Figure 6b) (Table 2).

Integration of reflection seismic data and seismicity

A carefully selected 2D seismic reflection profile (AV01) was reprocessed and reinterpreted (Figure 8). The reason behind the selection of this 2D seismic profile, in particular, is that it crosscuts the aftershock plane in a perpendicular direction, which delineates the M_L 5.5 rupture plane. Here, the 2D seismic data was interpreted with the main focus on regional structural geology and the structure that hosts the M_L 5.5 earthquake. In addition, we used the geological core logging and geophysical borehole logging data from the Moab Khotsong mine drilled by the ICDP-DSeis team (specifically drilled to intersect the M_L 5.5 rupture). These data were integrated and used to constrain the reflection seismic data interpretation.

Imperative to the study, critical stratigraphic markers, such as the base of the Transvaal Supergroup (2.6 Ga) were identified. This boundary was previously resolved through borehole observations and 3D reflection seismic data interpretation by Watts (2005). We could also detect the Ventersdorp Supergroup-Witwatersrand Supergroup boundary due to the acoustic impendence contrast between the overlying basalts and underlying quartzites of the upper Witwatersrand Supergroup Figure 8).

Structurally, the area is disturbed with multiple sub-vertical faults that tend to branch (Figure 8). Most importantly, the seismic section shows the delineation of the fault (yellow arrows in Figure 9) that correlates well with the seismogenic zone as defined by the aftershocks. The seismic section also exhibits strong and laterally continuous seismic reflections across the fold of seismic data, especially above the seismogenic zone at the cut-off of the aftershock plane (Figure 8 and Figure 9). These may be attributed to the presence of sills as described by Nkosi et al. (2022). These sills may be responsible for the sharp termination of the aftershocks. Furthermore, the section is characterised by low amplitude attenuated near-vertical structures, which may be interpreted as dykes (Figure 8 and Figure 9). The faulting (yellow arrows in Figure 9) shows vertical displacement – predominately reverse faulting (thrusting), which is also widely reported in the Witwatersrand Basin literature (Manzi et al., 2012a) (Figure 9).

Analysis and discussion

Dykes often intrude fault planes over lengths of up to several

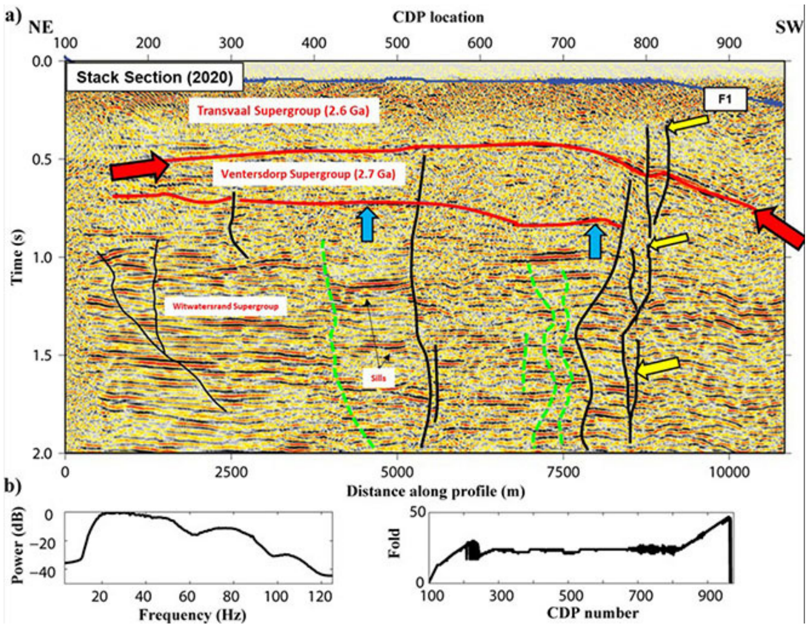

Figure 8—(a) The reprocessed legacy 2-D reflection seismic data (AV01) showing stratigraphic markers such as the Transvaal Supergroup and Ventersdorp Supergroup, e.g., red arrows show the stratigraphic marker; and Ventersdorp Supergroup and Witwatersrand Supergroup, e.g., blue arrows show the stratigraphic marker. The structures are marked clearly, and faults are shown in black, e.g., yellow arrows, while dykes are shown in green. The fault hosting the M_L 5.5 earthquake is indicated by F1. (b) The power spectrum of the processed seismic data (left) showing the dominant frequency of the data and the seismic fold of coverage (right)

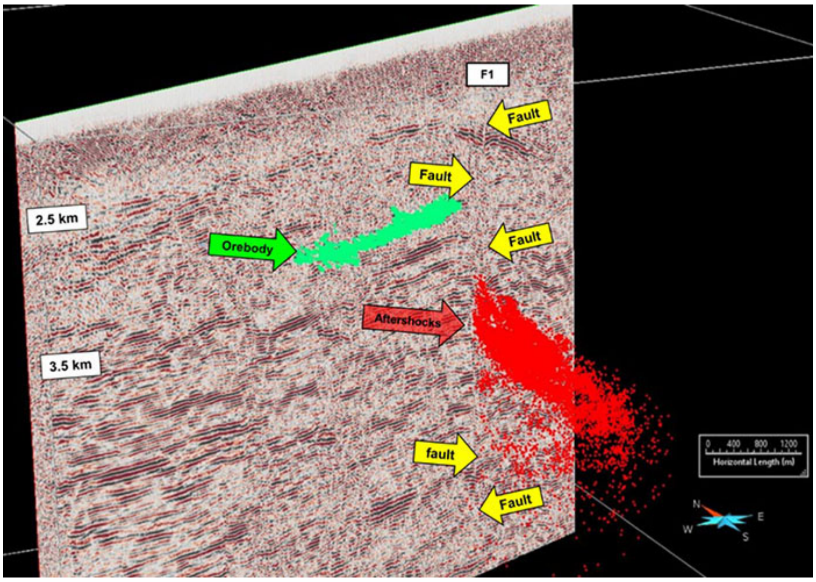

Figure 9—The seismic section extracted from the legacy 3-D reflection seismic data shows the mining stopes (green), fault structure (namely F1) that hosted the M_L 5.5 earthquake and seismicity data (red) (aftershocks)

kilometres, e.g., 15-16 km (Van der Heever, 1982). Watts (2005) and Van der Heever (1982) observed that the lamprophyre dykes are the youngest generation of igneous intrusive rocks in the Klerksdorp goldfields (Watts, 2005; Van der Heever, 1982). These dykes are often water- and methane-bearing and are associated with seismicity, which poses a risk to workers, mining operation, and infrastructure (Van der Heever, 1982). Van der Heever (1982) further observed that these dykes are soft, incoherent, and do not form strong, rigid transgressive bodies (Van der Heever, 1982). In general, the conditions in the research area are analogous to those reported by Van der Heever (1982). The ICDP-DSeis team drilled three holes (Holes A, B, and C) into the M_L 5.5 earthquake rupture delineated by the in-mine seismic network. Hole B and Hole C intersected dolerite sills and altered lamprophyre dykes (Rickenbacher, 2018), whereas Hole A intersected saline water (~10 MPa at the packer) that Onstott and the geomicrobiologist team were able to collect (Ogasawara et al., 2020).

As reported by Van der Heever (1982), Hole B demonstrates that the dyke is associated with the fault rupture zone and may be the source of weakness because it intersected the uppermost portion of the M_L 5.5 rupture zone, lamprophyre dyke, and experienced a 3 m core-loss zone. These events also coincided with the location of the aftershock for the M_L 5.5 rupture plane. These dykes are described by Van der Heever (1982) as having varying thicknesses ranging from around 1 m to over 3 m, striking northerly, and dipping almost vertically. Importantly, these geometric features match those seen in the reprocessed 2D reflection seismic section data as well as aftershock data. The M_L 5.5 earthquake fault mechanism is strike-slip and strikes in a NNW-SSE direction, as shown by Imanishi et al. (2017), who were able to observe the sharp termination of aftershocks right below the mining levels.

The Dseis core that was retrieved from drill holes contained dolerite sills and lamprophyre dykes. Near-vertical low amplitude structures and high amplitude horizontal reflectors were visible in the 2D reflection seismic section. Following an in-depth analysis of the drill core and 2D seismic section, it was determined that the horizontal high amplitude reflectors were dolerite sills intersecting the near vertical structure, and the near-vertical low amplitude structures were lamprophyre dykes associated with the fault hosting M_L 5.5. These structural elements may be responsible for the termination of the aftershocks below mining levels associated with the M_L 5.5 rupture. Yabe et al. (2019) measured the stress variations in the drill core successfully using the diametrical core deformation analysis (DCDA) stress-measurement method (Funato and Ito, 2017). The measurements revealed the localisation of stress in specific locations adjacent to: (1) the M_L 5.5 rupture in Hole B (intrusive rocks); (2) the upper edge of the aftershock region; and (3) the hypersaline brine fissure in Hole A (Yabe et al., 2019). It has been reported in the Bushveld Complex that these lamprophyre dykes are associated with rock failure through decomposing and gas outbursts (Daya, 2019). Large damaging seismic events tend to occur where sills and dykes intersect (Van der Heerver, 1982). Since dykes naturally intrude on mechanically weak areas, like faults, they are frequently linked to stress concentration over time that exceeds fault strength and trigger fault reactivation. This may describe the M_L 5.5 earthquake.

Fault gouges, their mineralogy, and the generation of wear material between two sliding rock surfaces have a major impact on slip weakening and rupture propagation (Zoback et al., 2011). Using gouge material collected from the M_L 5.5 rupture, we conducted friction experiments at slip velocity of 100 mm/s and a normal stress of 2 MPa. The Moab Khotsong gouge sample showed the peak friction coefficient of ~1.0, which decreased to steady-state friction of ~0.66 over a slip weakening distance of ~9.1 m. These friction coefficient values and weakening behaviour are similar to those found in Ortlepp shear fractures (Cooke 4 mine) at sub-seismic slip velocities (~100 mm/s) (Mngadi et al, 2021; Miyamoto et al., 2022).

The seismogenic zone at Cooke 4 mine is largely controlled by mechanical damage induced by mining-related stresses, while at Moab Khotsong mine, the study revealed that there may be three factors controlling the M_L 5.5 earthquake seismogenic zone: (a) intersection between lamprophyre dyke and dolerite sills, which creates a mechanical zone of weakness; (b) tectonic and/or mining-related stresses; and (c) chemical processes resulting from water and rock interaction.

Conclusion

Three holes, Hole A, Hole B, and Hole C (Figure 4), were drilled by the ICDP-DSeis team into the upper boundaries of the M_L 5.5 earthquake rupture. The team was able to develop the drilling chamber by excavating a section of a tunnel that was 2.9 km deep. Hole B intersected an altered lamprophyre dyke and encountered a core-loss zone using "double tube" core barrel. Due to the loss of the crucial core and fault gouge material, the team used a 1.5 m improved "triple tube" core barrel to drill a branch hole (Hole C). Fragile fault gouge material and core samples were successfully recovered. The aftershocks recorded by the in-mine seismic network delineated the M_L 5.5 rupture plane, and that corresponded with the location as the lamprophyre dyke and core-loss zone in the drill core. This means the altered lamprophyre dyke is the geological structure that hosted the M_L 5.5 rupture. Immediately after the drilling of Hole A, thorough core logging, downhole geophysics, physical property measurements, and non-destructive stress measurements were carried out. Furthermore, Onstott and the team of geomicrobiologists examined biomass, water, and gas, Nisson et al. (2023). The team detected and collected saline water successfully. Yabe et al. (2019) conducted non-destructive stress measurements and analysis on the recovered core from Hole A and found that the intrusive rocks, the top portion of the aftershock plane, and saline water were all associated with high stress concentration. Seismic velocity and density measurements, as well as geophysical borehole logging, revealed that intrusive rocks have high seismic velocities and density. Accordingly, intrusive rocks are expected to have a higher acoustic impendence contrast to country rocks. This is specific to dolerite sills, not highly altered lamprophyre dykes. The 2D legacy seismic data acquired in 1992 for gold exploration was reprocessed and reinterpreted. The reprocessing mapped high amplitude horizontal reflectors and a low amplitude near-vertical structure. The horizontal high amplitude reflectors were interpreted as dolerite sills that intersected the near vertical structure. When integrating the aftershock data from the in-mine seismic network, it was evident that the M_L 5.5 rupture plane was delineated by these aftershocks. This agreed with the near-vertical fault imaged by the 2D seismic reflection data, which showed a low-amplitude near-vertical structure. This was interpreted to be an altered lamprophyre dyke hosting the M_L 5.5 rupture. Furthermore, a strike-slip faulting mechanism that strikes NNW-SSE was revealed by the aftershock data.

Slip weakening and rupture propagation are significantly impacted by fault gouges, their mineralogy, and the production of wear material between two sliding rock surfaces. We performed friction experiments using gouge material extracted from the M_L 5.5 rupture at a normal stress of 2 MPa and a sub-seismic slip velocity of 100 mm/s. Over a slip weakening distance of approximately 9.1 meters, the Moab Khotsong gouge sample's peak friction coefficient of ~1.0 decreased to a steady-state friction of approximately 0.66. According to Mngadi et al. (2021), these friction coefficient values and weakening behaviour are comparable to those observed in Ortlepp shear fractures at sub-seismic slip velocities. This research study concludes that the M_L 5.5 earthquake rupture is complex, and that three or more factors control the seismogenic zone: (1) the intersection of dolerite sills and a lamprophyre dyke; (2) stresses related to tectonics and/or mining; and (3) chemical processes triggered by the interaction of water and rock formations.

Acknowledgments

Harmony Gold Mining Company Limited and Sibanye Gold Limited are acknowledged for providing permission to publish the results. The authors thank the School of Geosciences and the School of Mining Engineering at the University of the Witwatersrand, Wits Seismic Research Centre, Council for Geosciences, CIMERA, Ritsumeikan University, the CSIR Centre for Mining Innovation, JST-JICA, SATREPS team, ICDP DSeis team for the use of their resources and facilities. This project was also funded by JSPS KAKENHI grants 21224012, 21246134, 26249137, the MEXT's Earthquake and Volcano Hazards Observation and Research

Program, and the Earthquake Research Institute, the University of Tokyo cooperative research program. RJD acknowledges the support of the South African Research Chairs Initiative of the Department of Science and Technology and National Research Foundation. HO jr thanks UN University GLTP program.

References

Akimasa, I. 2018. Stress measurements with the Diametrical Core Deformation Analysis in the seismogenic zones of M2-5.5 earthquakes. method. Master Thesis, Ritsumeikan University. pp. 67–20

Coward, M.P., Spencer, R.M., Spencer, C.E. 1995. Development of the Witwatersrand Basin, South Africa. In: Coward, M.P., Ries, A.C. (Eds.). Early Precambrian Processes. *Geological Society*, London, Special Publications, vol. 95, pp. 243–269.

Dankert, B.T., Hein, K.A.A. 2010. Evaluating the structural character and tectonic history of the Witwatersrand Basin. *Precambrian Research*, vol. 177, pp. 1–22.

Daya, P. 2019. The petrology and petrogenisis of lamprophyric dykes in the Bushveld Complex, and their possible role in causing gas outbursts. University of the Witwatersrand. https://hdl.handle.net/10539/29293

Durrheim, R.J., Ogasawara, H., Nakatani, M., Yabe, Y., Kawakata, H., Naoi, M., Ward, A.K., Murphy, S., Wienand, J., Lenegan, P., Milev, A.M., Murakami, O., Yoshimitsu, N., Kgarume, T., Cichowicz, A., JST-JICA SA research group. 2012. Establishment of SATREPS experimental sites in South African gold mines to monitor phenomena associated with earthquake nucleation and rupture. *Proceedings of the 6th International Congress on Deep and High Stress Mining*. Perth, pp.173–187.

Funato, A., Ito, T. 2017. A new method of diametrical core deformation analysis for in-situ stress measurements. *International Journal of Rock Mechanics and Mining Sciences*, vol. 91, pp. 112–118. https://doi.org/10.1016/J.IJRMMS.2016.11.002

Gumsley, A., Stamsnijder, J., Larsson, E., Söderlund, U., Naeraa, T., de Kock, M., Sałacińska, A., Gawęda, A., Fabien Humbert, F., Ernst, R. 2020. Neoarchean large igneous provinces on the Kaapvaal Craton in southern Africa re-define the formation of the Ventersdorp Supergroup and its temporal equivalents. *Geological Society of America Bulletin,* vol. 132, pp. 9–10. https://doi: 10.1130/B35237.1

Hirono, T., Asayama, S., Kaneki, S., Ito, A. 2016. Preservation of amorphous ultrafine material: A proposed proxy for slip during recent earthquakes on active faults. *Scientific Reports*, 6, 36536.

Imanishi, K., Ogasawara, H., Yabe, Y., Horiuchi, S., Okubo, M., Murakami, O. 2017. Source parameters of the 2014 M_L 5.5 Orkney earthquake sequence, South Africa, estimated by using near-field underground seismic arrays in gold mines. IAG-IASPEI 2017. S02. Anthropogenic seismicity. 31 July 31, 2017.

Ishida, A., Sugimura, K., Liebenberg, B., Rickenbacher, M., Mngadi, S.B., Kato, H., Abe, S., Yabe, Y., Noda, T., Funato, A., Ito, T., Nakatani, M., Ward, A.K., Durrheim, R.J., Ogasawara, H. 2018. Stress measurement using cores of drilling into seismogenic zone of M2.0–M5.5 earthquakes in South African gold mines (ICDP DSeis project). *Japan Geosciences Union Meeting*, 20–24 May 2018, Chiba, Japan.

Kaneki, S., Yokoyama, Y., Hirono, T., Yabe, Y., Ogasawara, H. 2018. Mineralogical characteristics of fault rocks recovered from aftershock zone of the M_L 5.5 Orkney earthquake in South Africa (ICDP DSeis project). Seismological Society of Japan Fall Meeting, Abstracts.

Manzi, M.S.D., Gibson, M.A.S., Hein, K.A.A., King, N., Durrheim, R.J. 2012a. Application of 3D seismic techniques to evaluate ore resources in the West Wits line Goldfield and portions of the West Rand Goldfield, South Africa. *Geophysics*, vol. 77, WC163-WC171. https://doi:10.1190/GEO2012-0133.1

McCarthy, T.S., Rubidge, B. 2005. The Story of Earth and Life. Cape Town: Struik Publishers.

Midzi, V., Zulu, B.S., Manzunzu, B., Mulabisana, T., Pule, T., Myendeki, S., Gubela, W. 2015. Macroseismic survey of the M_L 5.5, 2014 Orkney earthquake. *Journal of Seismology*, vol. 19, no. 3. https://doi:10.1007/s10950-015-9491-2

Miyamoto, T., Hirono, T., Yokoyama, Y., Kaneki, S., Yamamoto, Y., Ishikawa, T., Tsuchiyama, A., Katayama, I., Yabe, Y., Ziegler, M., Durrheim, R.J., Ogasawara. H. 2022. Characteristics of Fault Rocks Within the Aftershock Cloud of the 2014 Orkney Earthquake (M_L 5.5) Beneath the Moab Khotsong Gold Mine, South Africa. *Geophysical Research Letters*, vol. 49, no. 14. https://doi:10.1029/2022GL098745

Mizoguchi, K., Hirose, T., Shimamot, T., Fukuyama, E. 2007. Reconstruction of seismic faulting by high-velocity friction experiments: An example of the 1995 Kobe earthquake. *Geophysical Research Letters*, vol. 34, L01308. https://doi:10.1029/2006gl027931

Mngadi, S.B., Durrheim, R.J., Manzi, M.S.D., Ogasawara, H., Yabe, Y., Yilmaz, H., Wechsler, N., Van Aswegen, G., Roberts, D., Ward, A.K., Naoi, M., Moriya, H., Ishida, A., SATREPS team and ICDP DSeis team. 2019. Integration of underground mapping, petrology, and high-resolution microseismicity analysis to characterise weak geotechnical zones in deep South African gold mines. *International Journal of Rock Mechanics and Mining Sciences*. vol. 114, pp. 79–91. https://doi.org/10.1016/j.ijrmms.2018.10.003

Mngadi, S.B., Tsutsumi, A., Onoe, Y., Manzi, M.S.D., Durrheim, R.J., Yabe, Y., Ogasawara, H., Kaneki, S., Wechsler, N., Ward, A.K., Naoi, M., Moriya, H., Nakatani, M. 2021. The effect of a gouge layer on rupture propagation along brittle shear fractures in deep and high-stress mines. *International Journal of Rock Mechanics and Mining Sciences*, vol. 137, pp. 1365–1609. https://doi.org/10.1016/j.ijrmms.2020.104454

Myers, R.E., McCarthy, T.S., Stanistreet, I.G. 1989. A tectono-sedimentary reconstruction of the development of the Witwatersrand Basin, with particular emphasis on the Central Rand Group. *Economic Geology Research Unit*, vol. 216, pp. 497–540.

Nisson, D.M., Kieft, T.L., Drake, H., Warr, O., Sherwood Lollar, B., Ogasawara, H., Perl, S.M., Friefeld, B.M., Castillo, J., Whitehouse, M.J., Kooijman, E., Onstott, T.C. 2023. Hydrogeochemical and isotopic signatures elucidate deep subsurface hypersaline brine formation through radiolysis driven water-rock interaction. *Geochimica et Cosmochimica Acta*, vol. 340, pp. 65–84.

Nkosi, N.Z., Manzi, M.S.D., Westgate, M., Roberts, D., Durrheim, R.J., Ogasawara, H., Ziegler, M., Rickenbacher, M., Liebenberg, B., Onstott, T.C., DSeis Team. 2022. Physical property studies to elucidate the source of seismic reflectivity within the ICDP DSeis seismogenic zone: Klerksdorp goldfield, South Africa. *International Journal of Rock Mechanics and Mining Sciences*, vol. 155, 105082. https://doi.org/10.1016/j.ijrmms.2022.105082

Ogasawara, H., Durrheim, R.J., Yabe, Y., Ito, T., Van Aswegen, G., Grobbelaar, M., Funato, A., Ishida, A., Ogasawara, Jr. H., Mngadi, S.B., Manzi, M.S.D., Ziegler, M., Ward, A.K., Hofmann, G., Moyer, P., Boettcher, M., Dight, P., Ellsworth, W., Liebenberg, B., Wechsler, N., Onstott, T., Berset, N., DSeis Team. 2017. Drilling into Seismogenic Zones of M2.0 – M_L 5.5 Earthquakes from Deep South African Gold Mines (DSeis): Establishment of Research Sites. *Proceedings of the AfriRock International Symposium*. 30 September 2017 – 6 October 2017, Cape Town, South Africa.

Ogasawara, H Jr. 2018. Calibration of seismic velocity structure and structural-geological interpretation in the seismogenic zone of the Orkney M5.5 earthquake of 5 August 2014. Master Thesis, Ritsumeikan University. pp. 53.

Ogasawara, H., B. Liebenberg, M. Rickenbacher, M. Ziegler, V.H. Esterhuizen, T.C. Onstott, R.J. Durrheim, M.S.D. Manzi, S. Mngadi, Y. Yabe, H.Y. Ogasawara, S. Kaneki, E. Cason, J.G. Vermeulen, E. an Heerden, T. Wiersberg, M. Zimmer, C. Kujawa, R. Conze, G. van Aswegen, N. Wechsler, A.K. Ward, S. Enslin, S. Tau, M.S. Bucibo, and the DSeis Team. 2019. 2019 status report: Drilling into seismogenic zones of M2.0–M5.5 earthquakes in South African gold mines (DSeis project). *Proceedings of the 9th International Congress on Deep and High Stress Mining, Symposium Series S98, Southern African.* Institute of Mining and Metallurgy, pp. 375–384. https://doi:10.36487/ACG_rep/1952_28_Ogasawara

Rickenbacher, M. 2018. Geological and Geotechnical Rock Mass Model from two deep DSEIS boreholes drilled at Moab Khotsong. *Swiss Federal Institute of Technology Zurich*, MSc Thesis.

Robb, L.J., Meyer, F.M. 1995. The Witwatersrand Basin, South Africa: Geological framework and mineralization processes. *Ore Geology Reviews*, vol. 10, pp. 67–94.

SACS (South African Committee for Stratigraphy). 1990. South African Stratigraphy. (Kent, comp.). Lithostratigraphy of the Republic of South Africa, South West Africa/Namibia, and the Republics of Bophuthatswana, Transkei and Venda. *Handbook, Geology of South Africa*, p. 690.

Sammis, C., Osborne, R., Anderson, J., Banerdt, M., White, P. 1987. Self-similar cataclasis in the formation of fault gouge. P*ure and Applied Geophysics*, vol. 124, nos. 1–2, pp. 53–78.

Van Aswegen, G. 2007. Ortlepp Shears – dynamic brittle shears of South African gold mines. *Potvin, Y (Ed.) 1st Southern Hemisphere International Rock Mechanics Symposium*, 16–19 September, Perth, Western Australia. pp. 111–120.

Van der Heever, P. 1982. The Influence of Geological Structures on Seismicity and Rockburst in the Klerksdorp goldfields. MSc (Geology). University of Johannesburg. Retrieved from: https://ujdigispace.uj.ac.za/ (Access date: 19 July 2020).

Vermaakt, D.T., Chunnet, I.E. 1994. Tectono-sedimentary processes which controlled the deposition of the Ventersdorp Contact Reef within the West Wits Line. In: Anhaeusser, C.R. (Eds.). *Proceedings of the 15th Congress of the Council for Mining and Metallurgical Institutions*, vol. 3, pp. 117–130.

Yabe, Y., Abe, S., Ito, T., Ishida, A., Sugimura, K., Kanematsu, M., Higashi, M., Tadokoro, R., Ogasawara, H., Funato, A., Kato, H., Watson, B., Mngadi, S.B., Durrheim, R.J., Hofmann, G., Scheepers, L. 2019. In-situ stress around source faults of seismic events in and beneath South African deep gold mines', in W Joughin (ed.). *Proceedings of the Ninth International Conference on Deep and High Stress Mining*. The Southern African Institute of Mining and Metallurgy, Johannesburg, pp. 399–411.

Watts, M. 2005. Mark Watts Project. Anglo Gold Ashanti, pp. 104.

Zoback, M., Hickman, S., Ellsworth, W., SAFOD Science Team. 2011. Scientific Drilling Into the San Andreas Fault Zone – An Overview of SAFOD's First Five Years. Scientific Drilling, 11, pp. 14–28. ◆